# Gallium K-Edge EXAFS Study of GaN:Mg Films

Yung-Chung Pan*[a], Shu-Fang Wang[a], Wen-Hsiung Lee[a], Wei-Cherng Lin[a], Chen-Ke Shu[a], Chung-I Chiang[b], Chin-Hwa Lin[b], Horng Chang[b], Jyh-Fu Lee[c], Ling-Yun Jang[c], Deng-Sung Lin[d], Ming-Chih Lee[a], Wen-Hsiung Chen[a] , and Wei-Kuo Chen[a]

[a]Department of Electrophysics, National Chiao-Tung University, Hsin-Chu, Taiwan, 300, R.O.C

[b]Chung-Shan Institute of Science & Technology, Tao-Yuan, Taiwan, 325, R.O.C.

[c]Synchrotron Radiation Research Center, Hsin-Chu, Taiwan, 300, R.O.C.

[d]Institute of Physics, National Chiao-Tung University, Hsin-Chu, Taiwan, 300, R.O.C.

**Abstract**

Ga K-edge extended X-ray absorption fine structure (EXAFS) measurement was employed to investigate the local structure of GaN:Mg films grown by metalorganic vapor phase epitaxy (MOVPE) with various $Cp_2Mg$ dopant flow rates using both in-plane and out-of-plane polarization modes of X-ray. The near edge absorption spectra were found to depend on X-ray polarization strongly for undoped GaN sample and weakly to minutely for heavily Mg-doped and amorphous films. The results indicate Mg incorporation modifies the local structure around the absorber Ga atom and, hence, alters the molecular orbital electron transition of GaN sample. EXAFS analysis showed both vacancy and Mg-interstitial defects contribute to the reduction of coordination numbers along the hexagonal *c*-axis of GaN:Mg film.

**Keyword** : EXAFS, GaN:Mg, MOVPE, polarization, structure, vacancy, interstitial

---

*Correspondence : E-mail : u8321810@cc.nctu.edu.tw ; Telephone : 886-3-5712121 ext 24426 ; Fax : 886-3-5725230

## 1. INTRODUCTION

With wide direct band gap and thermal stability, group III-nitride have continuously found applications in short-wavelength light-emitting and detecting, as well as high-temperature and high-power electronic devices.[1-2] The development of GaN-based devices, such as the brightness blue and green LEDs[3] and CW blue LDs[4], have achieved significant breakthrough. However, there still remains many problems for manufacturing high-quality GaN materials. The activation mechanism is one of the important issues for *p*-GaN. Mg dopant can be activated electrically to *p*-type performance by additional thermal process, such as low energy electron beam irradiation (LEEBI)[5] and thermal annealing (TA)[6]. However, it is still hard to obtain hole density higher than $10^{18}\,cm^{-3}$ in commercial *p*-type epilayer. It is important for Mg impurity to occupy right site to enhance *p*-type conductivity. Owing to about 10%-radius difference between Mg and Ga[7], a strong local lattice distortion can be expected once a Ga atom is replaced by Mg. Recent study of Si-doped GaN has shown that Si is not randomly distributed in the epilayer using polarized extended X-ray absorption fine structure (EXAFS).[8] In order to investigate problems of Mg-doped *p*-GaN, we also examined our samples with EXAFS measurement. Analyzing and simulation towards the understanding of the effect of Mg doping on the native defect population and the local microstructure around the Ga atom in epitaxial GaN were then followed.

## 2. EXPERIMENTIAL

All Mg-doped GaN samples (thickness ~0.5-1 μm) used in the experiment were grown on (0001) $Al_2O_3$ substrate by metalorganic vapor phase epitaxy (MOVPE) in atmospheric pressure. Trimethylgallium (TMGa), ammonia ($NH_3$), and biscyclopentadienylmagnesium ($Cp_2Mg$) were used as the Ga, N, and Mg sources, respectively. The carrier gas was purified nitrogen. Prior to the epilayer growth, the substrate was preheated for 10 minutes at 1,100℃, nitridated for 2 minutes at 1,050℃ and then cooled down to 520℃under about 1 slm ammonia flow for the deposition of GaN nucleation layer of about 400Å-thickness. The GaN:Mg epitaxial layer was grown at 1,075℃ using V/III ratio = 3,000 with $Cp_2Mg$ flow rate varying from 0 to 0.79 μmol/min.

In EXAFS experiment, the samples were oriented to have the hexagonal GaN c-axis either perpendicular or parallel to the electric field vector of the incident X-ray, corresponding respectively to in-plane (*i.e.* $\boldsymbol{E}$ field in *ab*-plane, or $\boldsymbol{E} \perp c$) and out-of-plane (*i.e.* $\boldsymbol{E}$ field along *c*-axis, or $\boldsymbol{E} \parallel c$) cases. Gallium K-edge EXAFS spectra were recorded at the wiggler beamline BL17C at Synchrotron Radiation Research Center (SRRC). The intensity of the incidence beam was measured by a $N_2$-filled ionization chamber as reference signal $I_o$ and the fluorescence emitted from the sample following the absorption of x-ray was measured by a Stern-Heald-Lytle detector with argon gas as the sampling signal $I_F$. The absorption coefficient $\mu$ is proportional to $(I_F/I_o)$. A Si(111) double-crystal monochromator with a 0.5 mm entrance slit was used for energy scanning. In order to record the spectra for Ga K-edge, a Zn-filter with thickness of 6 absorption length was placed between the sample and the window of the detector. Such an arrangement can efficiently lower the noise level resulting from the scattering of X-rays by the sample or the air.

## 3. RESULTS AND DISCUSSIONS

The intensity response of near edge X-ray absorption fine structure (NEXAFS) spectrum is very sensitive to the crystal group symmetry and the local structural around the central absorbing atom. The X-ray absorption cross section in an electric dipole approximation is given by

$$I \propto |\langle f|\boldsymbol{e}\cdot\boldsymbol{p}|i\rangle|^2 \propto (1/|\boldsymbol{E}|^2)|\langle f|\boldsymbol{E}\cdot\boldsymbol{p}|i\rangle|^2,$$

where $\boldsymbol{e}$ is a unit vector of the electric field vector $\boldsymbol{E}$, $\boldsymbol{p}$ is the electric dipole operator, $|i\rangle$ is the *1s* initial core level state and $|f\rangle$ is *2p* final conduction band states of the transition. For in-plane polarized synchrotron radiation ($\boldsymbol{E} \perp c$), the X-ray absorption spectrum shows the *ab*-plane crystalline information. On the other hand, for out-of-plane case ($\boldsymbol{E} \parallel c$), the spectrum revels more about the structural information along the crystal *c*-axis. Samples used in this report includes undoped (u-GaN), various content Mg-doped (GaN:Mg), and amorphous GaN (a-GaN).

Figures 1(a) and 1(b) show the Ga K-edge NEXAFS spectra of the three different GaN samples using respectively the $\boldsymbol{E} \perp$ *c*- and the $\boldsymbol{E} \parallel$ *c*-axis polarizations. It is found that the NEXAFS profiles of a-GaN are similar in both polarization modes because of their amorphous characteristic. On the other hand, dissimilarities of u-GaN and GaN:Mg NEXAFS spectra are seen in the two polarization modes. The anisotropic distribution of *p*-partial density of states (*p*-DOS) (final wave function, $|f\rangle$) in the conduction band between in *ab*-plane and along out-of-*ab*-plane (*c*-axis direction) is expected to consistent in a hexagonal crystal. It is further seen, the NEXAFS oscillation damped in the GaN:Mg case, in particularly, in $\boldsymbol{E} \parallel c$-axis polarization direction. This suggests that the influence of Mg impurity along *c*-axis direction is more serious than in *ab*-plane. Since our X-ray photon energy covers from 10200 to 11300 eV, it is sufficient to have EXAFS spectra analyzed. The routine pre-edge and atomic absorption subtraction followed by normalization to unit atom scale were performed with AUTOBK program for all samples. A typical Ga K-edge EXAFS spectrum from u-GaN in $\boldsymbol{E} \parallel c$-axis polarization, its corresponding *k*-space oscillation $\chi(k)$ (3.3-14 $Å^{-1}$), and Fourier Transform (F.T.) profile of GaN sample are showed in Fig. 2(a), 2(b), and 2(c), respectively. The processed experimental data were plotted in solid line and the fitting curves using FEFF program in dashes. They matched fairly well as can be seen from Figs. 2(b) and 2(c). From Fig. 2(c), the first and second strong features at ~1.6 and ~2.8 Å in the F.T. magnitude versus radical distance plots belong to the first-shell (Ga-N) and second-shell (Ga-Ga) contributions from a central Ga absorber, respectively. The FEFFIT fitting procedure was used to extract shell distances (R) and coordination numbers (N) for the nearest-neighbor shells adjacent to Ga atom for all GaN:Mg samples. The fitting results of $R_{Ga\text{-}N}$, $R_{Ga\text{-}Ga}$, $N_{Ga\text{-}N}$, and $N_{Ga\text{-}Ga}$ versus $Cp_2Mg$ flow rate from 0 to 0.79 μmol/min. are plotted in Figs 3(a), 3(b), 3(c), and 3(d), respectively. The amplitude reduction factor was fixed at 0.98 for all of the samples and calculated Debye-Waller factors always showing less than $7\times10^{-3}$ $Å^{-2}$.

In Figs. 3(a) and 3(b), the first-shell distance $R_{Ga\text{-}N}$ decreases only slightly and the second-shell $R_{Ga\text{-}Ga}$ increases also slightly as a function of Mg concentration around the values of ~1.95 and ~3.19 Å in both polarization modes, respectively. This trend agrees well with the results of N K-edge NEXAFS spectra, where the positions of the shape-resonance peaks shift in opposite directions as Mg concentration increases.[9] From the small variation of bond distances of the two shells, it can be deduced that crystalline structure remained in good quality even down to the heavy Mg-doped sample. In Figs. 3(c) and 3(d), however, show more noticeable change in coordination numbers for both polarization modes. These ~30%- and ~8%-

decreases respectively for the first-shell nitrogen and the second-shell gallium coordination numbers in *ab*-plane reflect a large amount of N- and Ga-vacancy defects were created during the Mg incorporation and the vacancy population was to vary with the flow rate. In additional to H passivation during the GaN epi-growth using $NH_3$ source, these vacancies may also passivate acceptors of as-grown *p*-GaN causing electrical property change and reducing carrier mobility. Neugebauer *et al.* argued both nitrogen and gallium vacancies, $V_N$ and $V_{Ga}$, are apt to be formed during the sample preparation due to their low formation energy.[10] It is known $V_{Ga}$ and $V_N$ act as shallow acceptors and donors, which, then, cause severe self-compensation effect and result in high resistivity in *p*-GaN. In addition to associating with Mg acceptors to lower the free hole carrier concentration, $V_N$ donors could also passivate $V_{Ga}$ acceptors to form scattering centers that increase impedance intensively. Therefore, the suppression of formation of these vacancy defects may be of essential and constitutes a key factor for good characteristic performance of *p*-type GaN.

It is also seen from Figs. 3(c) and 3(d), the first-shell $N_{Ga-N}$ appears to decrease less than the second-shell $N_{Ga-Ga}$ noticeably from 2.0 to ~0.75 and 6.0 to ~2.1 along the *c*-axis direction, respectively. Such a near by 65%-decrease of both coordination numbers definitely would damage the crystalline structure of hexagonal GaN epilayer and degrade the film properties. However, this speculation is not consistent with the results of good crystalline characteristics for GaN:Mg sample from the tendency of shell distances change as a function of Mg concentration. Consequently, these great decreases of first- and second-shell coordination numbers along the *c*-axis can not be explained solely by the formation of vacancy defects. Reboredo and Pantelides have suggested that, in addition to substitutional Mg ($Mg_{Ga}$) in $Mg_{Ga}$-N-H form, interstitial Mg ($Mg_i$) plays also a significant role for self-compensation of *p*-materials.[11] Therefore, in addition to $Mg_{Ga}$ there must be $Mg_i$ situated to provide acceptors and reduce the F.T. magnitude. These interstitial defects could also contribute crucially to the reduction of coordination numbers. As we have no direct data to confirm this, we simulated some possible cases for comparing to our data using both in-plane and out-of-plane polarizations. Figs. 4(a) and 4(b) show respectively the $k^3\chi(k)$ variation in *k*-space and the simulated F.T. magnitude in *R*-space of u-GaN (solid curve) and GaN:Mg with interstitial defect $Mg_i$ (dotted curve). Fig. 4(a) shows a phase shift of nearly $\pi$ between the simulated curves of the two samples near the low *k* region and in Fig. 4(b) the F.T. magnitude of the doped model decreases when interstitial $Mg_i$ are present in GaN film. Both indicate that interstitial defects would induce the cancellation of the amplitude of the corresponding F.T. oscillation and, hence, reduce the coordination numbers. The coordination number reduction was also reported in ZnSe:Cu II-XI compound sample, whose $Cu^{+2}$ occupy either at the zinc substitutional site ($Cu_{Ze}$) or at the interstitial site ($Cu_i$).[12] Therefore, we conclude that both Mg interstitial defects as well as N and Ga vacancies all favor to occur along the *c*-axis direction of the hexagonal GaN crystal and they collectively contribute to the reduction of coordination numbers along that direction.

## 4. CONCLUSION

The doping effect of GaN:Mg samples were investigated with Ga K-edge X-ray absorption spectroscopy. The data showed that NEXAFS profiles and the corresponding structural parameters have a strong anisotropic aspect between in *ab*-plane and along out-of-*ab*-plane (*c*-axis direction). Moreover, the neighboring shell distances and coordination numbers around Ga atom are very sensitive to the Mg concentration. The N- and Ga-vacancies were induced simultaneously during the

incorporation of Mg impurity, which caused coordination number reduction. However, a 65% decrease of coordination numbers along the *c*-axis direction was considered too large to be explained solely by vacancy formation. In addition to the substitutional $Mg_{Ga}$, simulation results based on interstitial $Mg_i$ model did show its contribution to the coordination number reduction. Those multiple induced defects were formed to appear along the *c*-axis direction favorably when examined with polarized EXAFS measurements.

## ACKNOWLEDGMENTS

The authors would like to thank the National Science of the Republic of China for the financial support of this research under contract numbers NSC88-2112-M-009-021, -022, and -031.

## REFERENCES

1. S. Strite and H. Morkoç, "GaN, AlN, and InN: A review," *J.V.S.T.* **B 10**, pp. 1237-1266, 1992.
2. H. Morkoc, S. Strite, G. B. Gao, M. E. Lin, B. Sverdlov, and M. Burns, "Large-band-gap SiC, III-V nitride, and II-VI ZnSe-based semiconductor device technologies," *J. Appl. Phys.* **76**, pp. 1363-1398, 1994.
3. S. Nakamura, M. Senoh, N. Iwasa, and S. Nagahama, "High-Brightness InGaN Blue, Green and Yellow Light-Emitting Diodes with Quantum Well Structures," *Jpn. J. Appl. Phys.* **34**, pp. L797-L799, 1995.
4. S. Nakamura, M. Senoh, S. Nagahama, N. Iwasa, T. Yamada, T. Matsushita, H. Kiyoku, Y. Sugimoto, T. Kozaki, H. Umemoto, M. Sano, and K. Chocho, "High-power, long-lifetime InGaN/GaN/AlGaN-based laser diodes grown on pure GaN substrates," *Jpn. J. Appl. Phys.* **37**, pp. L309-L312, 1998.
5. H. Amano, M. Kitoh, K. Hiramatsu and I. Akasai, "P-Type Conduction in Mg-Doped GaN Treated with Low-Energy Electron Beam Irradiation (LEEBI)," *Jpn. J. Appl. Phys.* **28**, pp. L2112-L2114, 1989.
6. S. Nakamura, N. Iwasa, M. Senoh, and T. Mukai, "Hole Compensation Mechanism of P-Type GaN Films," *Jpn. J. Appl. Phys.* **31**, pp. 1258-1266, 1992.
7. S.-G. Lee and K. J. Chang, "Atomic model for blue luminescences in Mg-doped GaN," *Semicond. Sci. Technol.* **14**, pp. 138-142, 1999.
8. Z. H. Lu, T. Tyliszczak, P. Broderson, A. P. Hitchcock, J. B. Webb, H. Tang, and J. Bardwell, "Local microstructure of Si in GaN studied by x-ray absorption spectroscopy," *Appl. Phys. Lett.* **75**, pp. 534-536, 1999.
9. Y.C. Pan, S. F. Wang, W. C. Lin, W. H. Lee, C. I. Chiang, H. Chang, H. H. Hsieh, J. M. Chen, D. S. Lin, M. C. Lee, W. K. Chen, and W. H. Chen, "Structure Study of GaN:Mg Films by Near Edge Absorption Fine Structure Spectroscopy and X-Ray Diffraction," to be published in *Jpn. J. Appl. Phys.*
10. J. Neugebauer and C. G. Van de Walle, "Atomic geometry and electronic structure of native defects in GaN," *Phys. Rev.* **B 50**, pp. 8067-8070, 1994.
11. F. A. Reboredo and S. T. Pantelides, "Novel Defect Complexes and Their Role in the *p*-Type Doping of GaN," *Phys. Rev. Lett.* **82**, pp. 1887-1890, 1999.
12. A. I. Goldman, E. Canova, Y. H. Kao, B. J. Fitzpatrick, R. N. Bhargava, and J. C. Philips, "Extended x-ray absorption fine structure studies of diffused copper impurities in ZnSe," *Appl. Phys. Lett.* **43**, pp. 836-838, 1983.

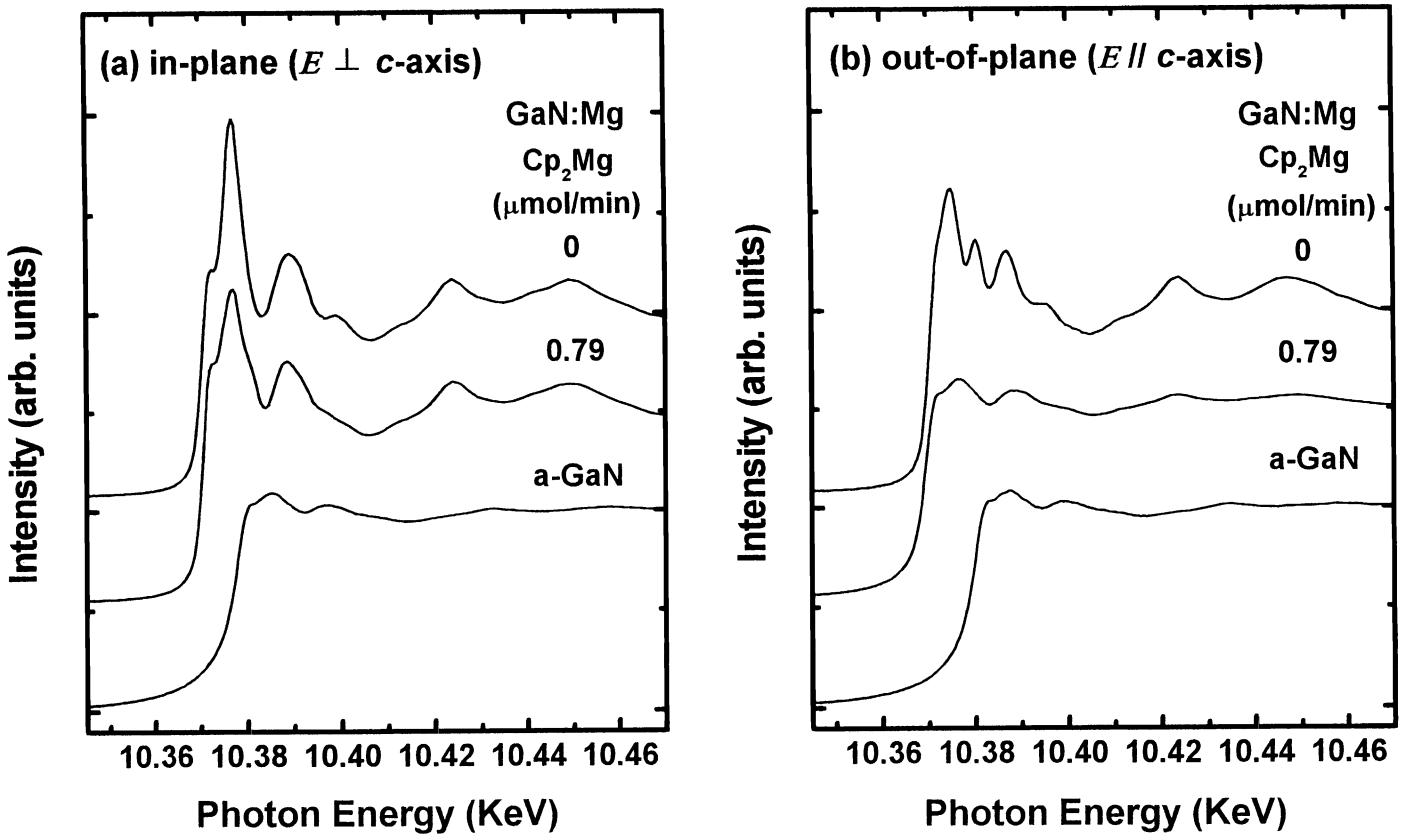


1. Ga K-edge NEXAFS spectra from undoped, Mg-doped, and amorphous GaN films for (a) in-plane ($\boldsymbol{E} \perp c$) and (b) out-of-plane ($\boldsymbol{E}$ // $c$) polarization modes.

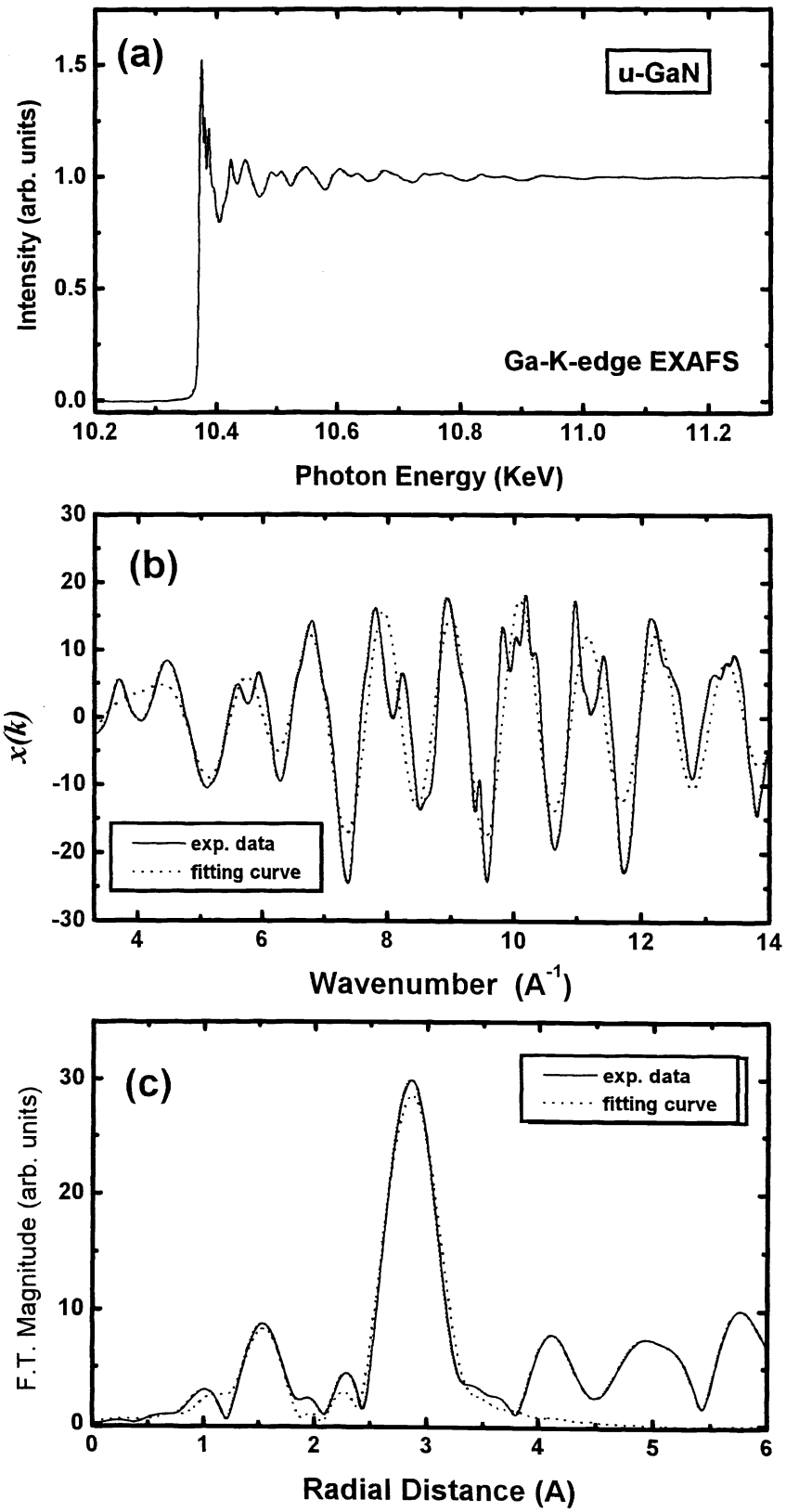


2. (a) Ga K-edge EXAFS spectrum, (b) corresponding $k$-space oscillation $\chi(k)$, and (c) Fourier Transform (F.T.) profile of u-GaN in $\boldsymbol{E}$ // $c$-axis polarization.

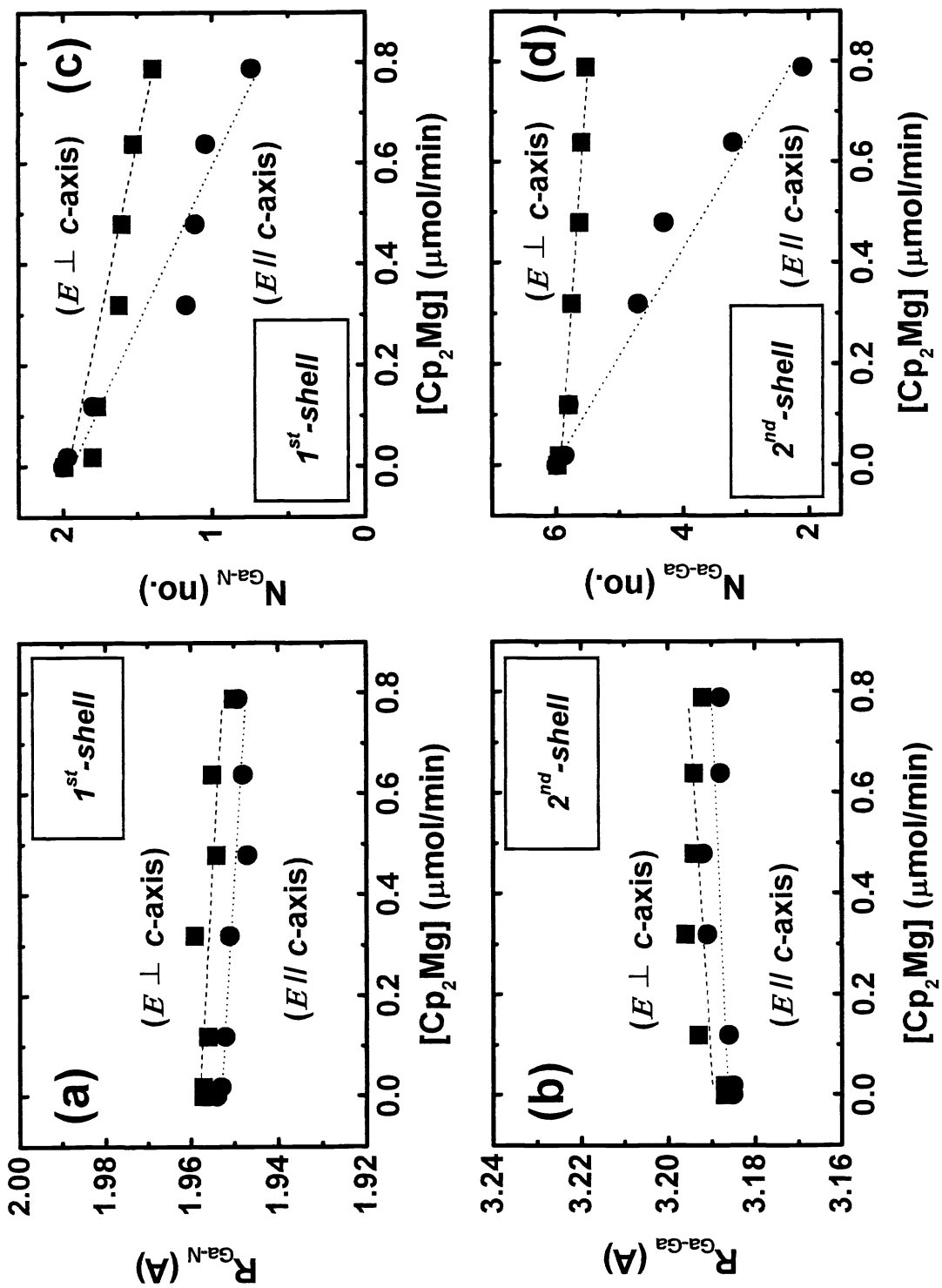


3. (a) The shell distances ($R_{Ga-i}$) and (b) the corresponding coordination numbers ($N_{Ga-i}$) of the first- (i=N) and the second- (i=Ga) shells for various Mg-doped GaN samples in both polarization modes.

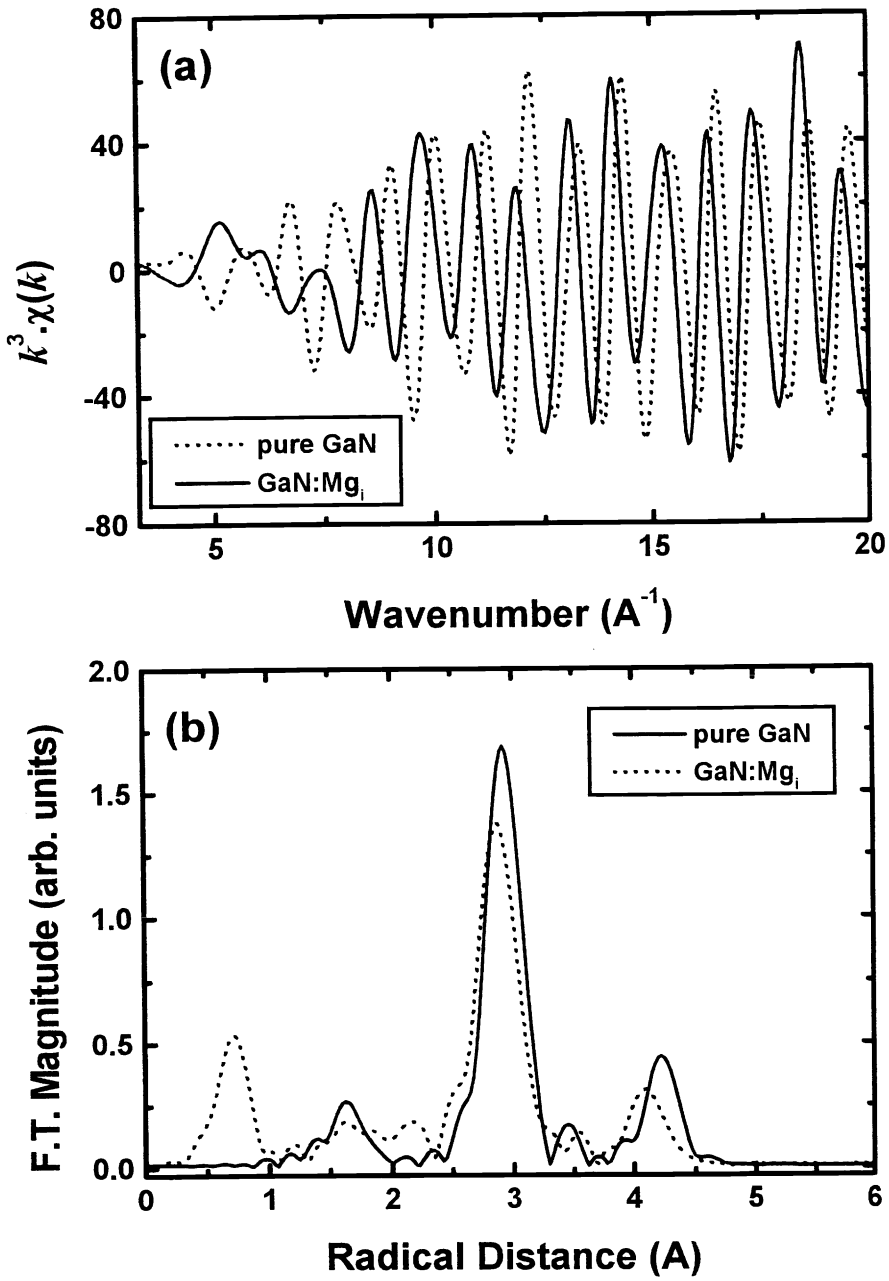


4. The simulated (a) *k*-space oscillation and (b) *R*-space F.T. profiles of undoped (solid curve) and Mg-doped (dotted curve) hexagonal GaN.